Cuadernos de Investigación Geográfica *Geographical Research Letters*	2025	Nº 51 (2)	pp. 85-108	EISSN 1697-9540

http://doi.org/10.18172/cig.6769

CONSEQUENCES OF FIRE ON VEGETATION COMPOSITION AND ITS INFLUENCE ON LEAF AREA INDEX (LAI) DISTRIBUTION USING MULTI-RESOLUTION IMAGES

PEDRO MARTÍN ORTIZ*, FERNANDO PÉREZ-CABELLO, CRISTIAN IRANZO CUBEL, RAQUEL MONTORIO LLOVERIA

Department of Geography and Land Management, University Institute of Environmental Sciences (IUCA), University of Zaragoza, Zaragoza, Spain.

ABSTRACT In recent decades, wildfires have become one of the main disturbances affecting Mediterranean forest ecosystems. Understanding how fire-affected formations recover is crucial for assessing their resilience and effectively managing potential hydrological-forest restoration measures. This study analyzes vegetation regeneration in burned areas representative of the landscape diversity of Aragón (NE Iberian Peninsula) considering (i) the type of colonizing vegetation in relation to the pre-existing one and (ii) the impact of the colonizing vegetation type on the spatial distribution of the Leaf Area Index (LAI), which is used as a proxy for the eco-physiological functionality of the affected formations. High-spatial-resolution GeoSAT-2 images and Sentinel-2 L2A collections were used to generate maps of current vegetation distribution and multitemporal LAI composites, respectively. Contingency tables derived from diachronic comparisons of dominant vegetation type (before the fire and at present) and Random Forest (RF) predictive models were employed. The RF models also determined the importance of different natural factors in the spatial distribution of colonizing vegetation formations. The results highlighted the strong dependence between pre-fire and colonizing vegetation formations (χ^2 = 10.067) and the role of regenerative trajectories in the spatial distribution of LAI ($p < 0.05$). Greater regeneration was observed in areas dominated by species with active reproductive strategies (resprouting and serotiny). Additionally, in the Random Forest modeling (OOB = 21%), pre-existing vegetation emerged as the most determining factor (MDG = 600) in predicting current vegetation, surpassing fire severity and the regenerative trend of the Normalized Difference Vegetation Index (MDG ≈ 250), whose effects vary depending on the type of vegetation formation.

Consecuencias del fuego en la composición de la vegetación y su influencia en la distribución del Leaf Area Index (LAI) mediante imágenes multi-resolución

RESUMEN. En las últimas décadas, los incendios forestales constituyen una de las principales perturbaciones de los ecosistemas mediterráneos. Comprender cómo se recuperan las formaciones afectadas es fundamental para evaluar su resiliencia y gestionar adecuadamente medidas de restauración hidrológico-forestal. Este estudio analiza la regeneración vegetal en zonas incendiadas representativas de la diversidad paisajística de Aragón (NE de la Península Ibérica), considerando (i) el tipo de vegetación colonizadora en relación con la preexistente y (ii) su impacto en la distribución espacial del Índice de Área Foliar (LAI), este último utilizado como proxy de la funcionalidad eco-fisiológica de las formaciones afectadas. Se hace uso de imágenes GeoSAT-2 de alta resolución espacial y colecciones Sentinel-2 L2A para obtener cartografías sobre la distribución de la vegetación actual y compuestos multitemporales de LAI, respectivamente. Se emplean tablas de contingencia derivadas de comparaciones diacrónicas del tipo de vegetación dominante (antes del fuego y en el momento actual) y modelos predictivos Random Forest (RF), que también han permitido determinar la importancia de diferentes factores naturales en la distribución espacial de las formaciones vegetales colonizadoras. Los resultados ponen de manifiesto la alta dependencia entre las formaciones vegetales previas y las colonizadoras (χ^2 = 10.067) y el papel de las trayectorias regenerativas en la distribución espacial del LAI ($p < 0.05$), observándose una mayor regeneración en áreas donde predominaban especies con estrategias reproductivas activas (rebrote y serotinia). Asimismo, en la modelización mediante Random Forest (OOB = 21%) la vegetación preexistente emerge como el factor más determinante (MDG = 600) en la predicción de la vegetación actual, por encima de la severidad del fuego y la tendencia regenerativa del *Normalized Difference Vegetation Index* (MDG ≈ 250), cuyos efectos varían en función del tipo de formación vegetal.

Keywords: Remote sensing, multispectral time series, post-fire resilience, fire severity, LAI.

Palabras clave: Vegetación, fuego, regeneración, teledetección, LAI.

Received 01 May 2025

Accepted 03 November 2025

***Corresponding Author:** Pedro Martín Ortiz, Department of Geography and Land Management, University Institute of Environmental Sciences (IUCA), University of Zaragoza, C/ Perdro Cerbuna, 12, 5009, Zaragoza, Spain. E-mail: pedro.martin@unizar.es

1. Introduction

In the current context of Aragon's forest ecosystems, as well as in most of those of the Mediterranean area, fires are one of the main environmental problems. This is due to an increase in their recurrence and intensity in recent decades (Moreno *et al.*, 2023; Ruffault *et al.*, 2020). Although fire has been presented throughout history as a natural landscape shaping element (Karavani *et al.*, 2018; Keeley, 2012), recent transformations in socioeconomic activities, land uses, as well as changes in weather patterns are modifying natural fire regimes (Bodí *et al.*, 2012), and even compromising the natural recovery of affected ecosystems (Lecina-Diaz *et al.*, 2021).

From an ecological-landscape perspective (Bodí *et al.*, 2012), the destruction of vegetation is the most immediate and far-reaching effect. However, after a forest fire there is an intense activity of regeneration mechanisms (Ne'eman *et al.*, 2004) of pre-existing species. These mechanisms largely determine the pace and intensity of the recovery process (Pausas, 2012) through adaptive mechanisms such as serotiny, regrowth or protection through bark thickness (Keeley, 1981; Pausas *et al*., 2017). Nevertheless, fire can alter landscape patterns in the medium or long term (Vallejo *et al.*, 2009; Vayreda *et al.*, 2016) and cause permanent changes in the floristic composition of the affected plant community. This is due to the degradation of soil´s physical and chemical properties, in which fire severity plays an important role (Keeley *et al.*, 2005; Muñoz-Rojas and Pereira, 2020).

In order to properly manage the affected areas, improve their conservation status, and protect them from further disturbance, it is essential to have information on how recovery is occurring (Cerdà and Robichaud, 2009; Ramos and Soares, 2004). In this context, monitoring vegetation response and establishing long-term diagnostic methods are essential (Martinez *et al*., 2017).

The products obtained through methodologies supported by orbital and airborne remote sensing have great potential at a regional scale, both in damage assessment and temporal monitoring of plant regeneration (Gitas *et al.*, 2012; Wagtendonk *et al.*, 2004; Woodgate *et al.*, 2024). There are numerous publications in the scientific literature that study the effects of fire on vegetation based on indicators and spectral metrics, or on algorithms capable of analyzing spatio-temporal variability (Griffiths *et al*., 2014). These works use images of widely varying spectral, temporal and spatial resolution (Woodgate *et al.*, 2024). Among the programs with high/moderate spatial resolution, Landsat collections have been the most widely used. This is due to their revisit period (16 days), high spatial resolution (30 meters), and the fact that they go back more than 5 decades over time (Wulder *et al*., 2022). NDVI *(Normalized Difference Vegetation Index*) has been one of the most widely used indices among the spectral indicators, as it reflects changes in leaf area and total biomass (Henry and Hope, 1998). In addition, its ease of collection and the possibility to track it over time make this index a useful tool for analyzing regeneration from an evolutionary perspective.

The use of parameters such as the *Leaf Area Index (LAI)* provides estimates of vegetation biophysical properties (Pettorelli *et al.,* 2005) that could also be employed as indicators of the degree of post-fire recovery or affection (Jiménez *et al*., 2016). *LAI*, a structural property of the canopy, refers to the amount of vegetation distributed vertically and is defined as the photosynthetically active leaf area per unit of ground (Chen and Black, 1992). For large areas, it can be estimated by remote sensing (Li *et al.*, 2022; Pu *et al.*, 2024). In this context, the use of bio processors applied to Sentinel-2 images within the Copernicus Earth Observation Program represents an internationally prominent example (Juola *et al.*, 2024; Korhonen *et al.*, 2017).

Although spectral information can highlight specific aspects of the forest canopy, identifying the type of formation based on the main species (composition) remains fundamental to studying burned areas using satellite images (Shanmuga and Vani, 2024). Digital classification techniques applied to multispectral data have been widely used for mapping, change detection and canopy monitoring (Rogan and Chen, 2004; Choudhury *et al.*, 2020; Chaves *et al.*, 2020). High spatial resolution images are especially useful because they allow for the accurate and detailed identification of vegetation (Ancira-Sánchez and Treviño, 2015). Additionally, multi-scale and multi-temporal approaches are necessary to detect the various phenological aspects that characterize different vegetation types (Simonetti *et al.*, 2015; Vogelmann *et al.*, 2012).

The availability of different diagnostic indicators of the regeneration process makes it possible to analyze the different role played by factors such as fire characteristics in terms of severity or the reproductive strategy of the pre-existing vegetation. In this context, the development of predictive models is essential to understand the complex interactions between these variables and their influence on post-fire vegetation formations (Viana-Soto *et al.*, 2020). There are many studies in the literature that follow this line of research. They often establish rankings or hierarchies of predictors, determining the specific role that each of them plays in ecological regeneration (Basset *et al.*, 2017; Chu *et al.*, 2017). However, such evaluations often involve analyzing the indicators individually rather than integrating them as a whole.

The objective of this work is to analyze the magnitude of vegetation regeneration in terms of composition (replacement of pre-existing vegetation formations) in representative areas of Aragon landscapes affected by forest fires. Additionally, it intends to determine how the type of vegetal species that regenerates after the fire influences the spatial distribution of LAI levels. Additionally, the study aims to analyze the influence of fire severity and temporal trends on regeneration processes.

This required (i) identifying current vegetation formations using high spatial resolution multispectral images and evaluating recovery in relation to pre-existing formations (trajectories); (ii) analyzing the spatial distribution of LAI values in each of the fires and in relation to the trajectories; and (iii) developing predictive models for the evolution of vegetation composition in the affected areas, establishing the explanatory factors that contribute to vegetation regeneration and the current state of the composition.

2. Study Area

The study area was limited to four representative forest fires (Seira, Pico del Águila, Montes de Zuera, and Aliaga), with an average area of approximately 3,000 ha, occurring in different years (1986, 1991, 1995, and 2008) (Fig. 1). These fires were distributed along a transect encompassing part of the biogeographic and landscape variability of Aragón, following the cartography of the Great Landscape Domains [Atlas of Aragon (ICEARAGON), n.d.] and the Vegetation Series of Spain (Rivas-Martínez, 1987).

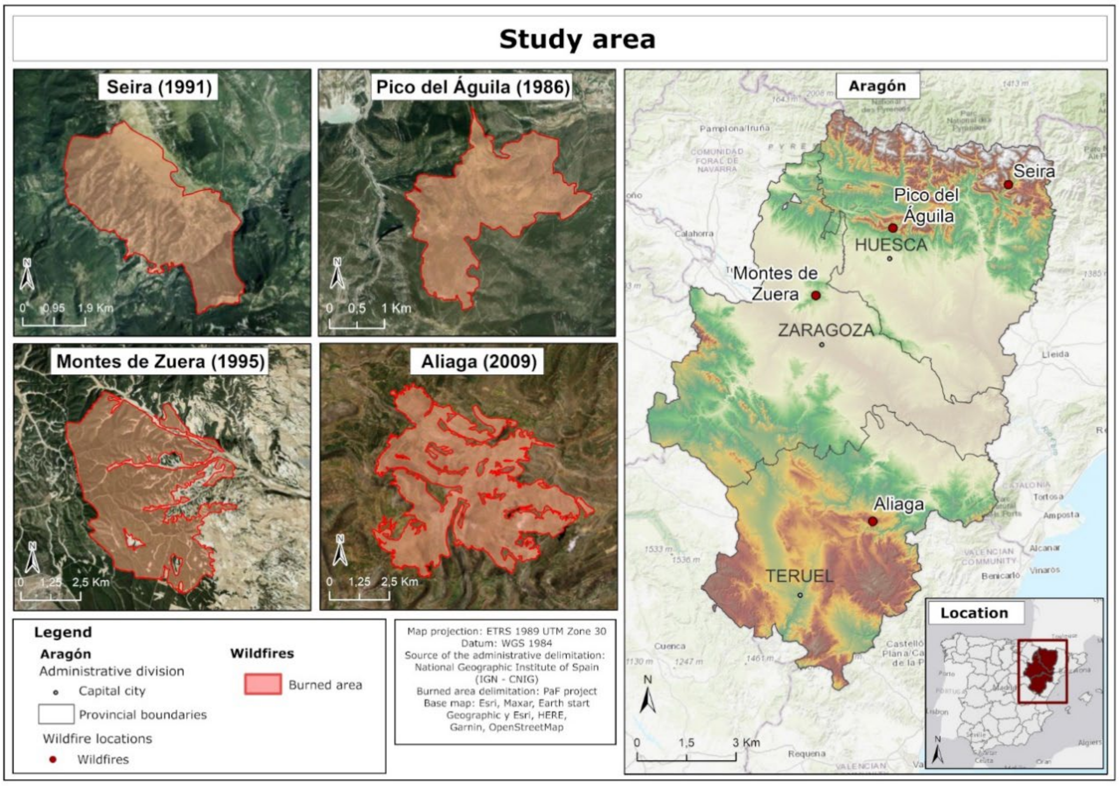

Figure 1. Study area: perimeters of burned areas and location in the regional context of Aragon.

The Seira fire occurred in August 1991 (~1,800 ha) and was located in the Sierra de Chía, near the Ésera River, within the domain of the High-Mountain Calcareous Pyrenean Massifs and the Silver Fir pine series. The Pico del Águila fire, which took place in August 1986 (~500 ha) in the southeastern part of the eponymous range, falls within the domain of the Medium-Mountain Calcareous Pyrenean Ranges and the potential Quercus ilex (holm oak) series. The Zuera Mountains fire, from 1995 (~3,000 ha), is included in the domain of the Calcareous Ranges of the Ebro Depression and the holm oak series. Finally, the Aliaga fire, occurring at the end of July 2009 (~6,300 ha), was located within the major landscape domains of the Medium-Mountain Calcareous Iberian Ranges and in the potential holm oak vegetation series.

The selection of these areas was conducted through a systematic process designed to identify representative forest fires with contrasting characteristics. The methodological details of this selection procedure are provided in the corresponding Materials and Methods section.

3. Materials and Methods

The methodological process followed to analyze the recovery level of plant communities affected by fire from an eco-physiological approach and at the plant formation level, is based on three main work phases (Fig. 2): (i) selection of representative fires of the biogeographic variability of Aragon; (ii) obtaining diagnostic variables related to the recovery state of forest fires. This includes digital classification processes of satellite images, trend analysis of multispectral indices (NDVI), and obtaining biophysical parameters (LAI); (iii) predictive modeling of the degree of recovery of plant formations from the point of view of the dominant species using Random Forest (RF).

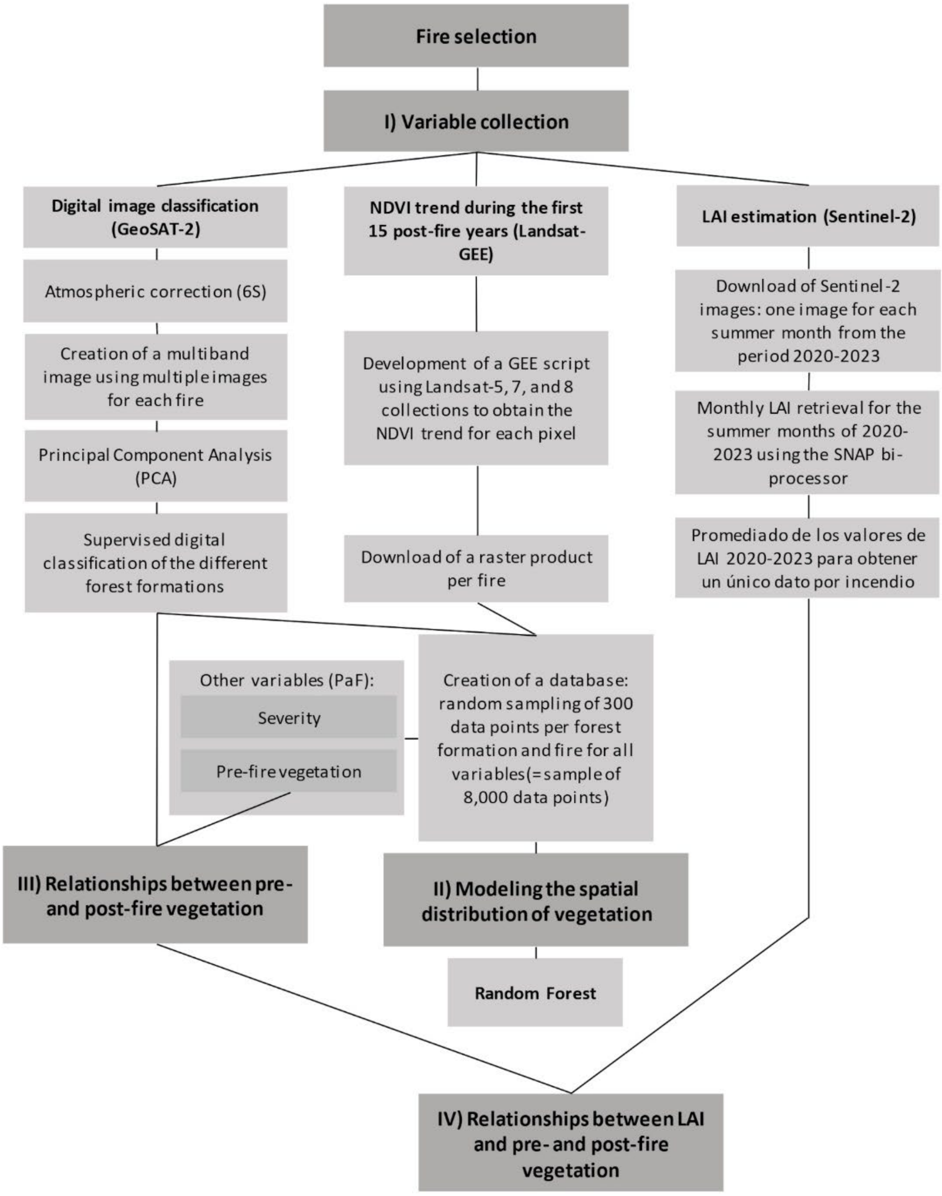

Figure 2. Methodological framework.

3.1. Materials

3.1.1. Satellite images

3.1.1.1. Spatial distribution of plant formations in the burned areas

GeoSAT-2 is a very high spatial resolution Earth observation satellite (3 m in multispectral and 0.75 m in panchromatic) that records quadrangle scenes of 12 km lateral surface. These scenes consist of four multispectral bands, three in the visible (VIS: 0.40 - 0.75 µm) and one in the near infrared (NIR: 0.75 - 1.30 µm), in addition to a panchromatic image. In this study, we specifically used 10 *Bundle* (L1C) products that cover the largest portion of the burned area in the analyzed fires. The description and technical characterization of the images can be found in the GeoSAT technical manual provided by the *Instituto Geográfico Nacional* (2021). The images were obtained from the General Action Protocol between IGN (*Instituto Geográfico Nacional*) /CNIG (*Centro Nacional de Información Geográfica*) and CDTI (*Centro para el Desarrollo Tecnológico y la Innovación*). Copyright © GEOSAT.

3.1.1.2. Sentinel-2 images: Spatial distribution of LAI values in burned areas

The products of ESA's Sentinel-2 (S2) mission used in this work are multispectral L2A satellite images, i.e., images that have undergone an atmospheric correction process to obtain the reflectance in the lower part of the atmosphere (Bottom Of Atmosphere -BOA). These images were downloaded from the Copernicus data platform, and correspond to the period 2020-2023. For each year, an image representative of the summer months in the northern hemisphere (June, July and August) was selected. In total, 12 different S2 images were used for each fire. The LAI values were calculates using these images.

3.1.1.3. Landsat image collections: Trend analysis of NDVI values

A temporal analysis of the NDVI index was performed using Landsat images (5, 7, and 8) from Collection 2, Level 2 (C2 L2). This collection provided atmospherically corrected surface reflectance and land temperature products using the LEDAPS (Landsat Ecosystem Disturbance Adaptive Processing System) and LaSRC (Land Surface Reflectance Code) algorithms for optical sensors. The NDVI trend was obtained through *Google Earth Engine* (GEE), a cloud processing platform designed for the analysis of geospatial data on a global scale (Gorelick *et al.*, 2017). We considered a 15-year period following the dates of the fires.

3.1.2. Pre-vegetation and severity mapping

In order to know the spatial distribution of pre-fire vegetation in the selected areas and the severity of fire, we used cartographic products. These were obtained from the digital classification of Landsat multispectral images (Iranzo Cubel *et al.*, 2023) and the calculation of the RdNBR *(Relative differenced Normalized Burn Ratio*) index (Miller and Thode, 2007; Montorio *et al*., 2024), both developed within the framework of the "PaF" project. These products provided detailed information, with a spatial resolution of 30 m, on the various forest formations that occupied the areas affected by the fire, as well as a short-term approximation of the spatial distribution of fire severity.

3.2. Methods

3.2.1. Fire selection

Representative fires were selected using a probabilistic Gaussian Mixture Model (GMM) (Xuan *et al.,* 2001), which identifies subpopulations by combining multiple Gaussian distributions. The probability that fires in Aragon (>100 ha, 1985-2015; Forest Fire Database of the Government of Aragon, General Directorate of Forest Management) belonged to each group was estimated, and each fire was assigned to the group with the highest probability. Model parameters were optimized using the Expectation–Maximization (EM) algorithm, which iteratively calculates membership probabilities and adjusts parameters to maximize overall likelihood.

The GMM method was applied to three distinct sets of criteria pairs: (1) geographic distribution -longitude and latitude; (2) topographic altitude and solar radiation; (3) severity (average of each fire) and area burned in each event. The DTMs (Digital Terrain Models) used were downloaded from the *Centro Nacional de Información Geográfica* (CNIG-IGN), and a solar radiation analysis was applied on them, deriving a raster with values of watt-hours per square meter (ESRI ArcMap). For operational reasons, the number of analyzed fires was reduced, selecting those that generally represented the diversity of forest landscapes affected by fire in Aragon. In addition, the availability of Geosat-2 images and field data was taken into account.

Figure 3 presents the distribution of fires across three bivariate scenarios, revealing distinct clustering patterns. The four fires analyzed are considered representative cases of these patterns.

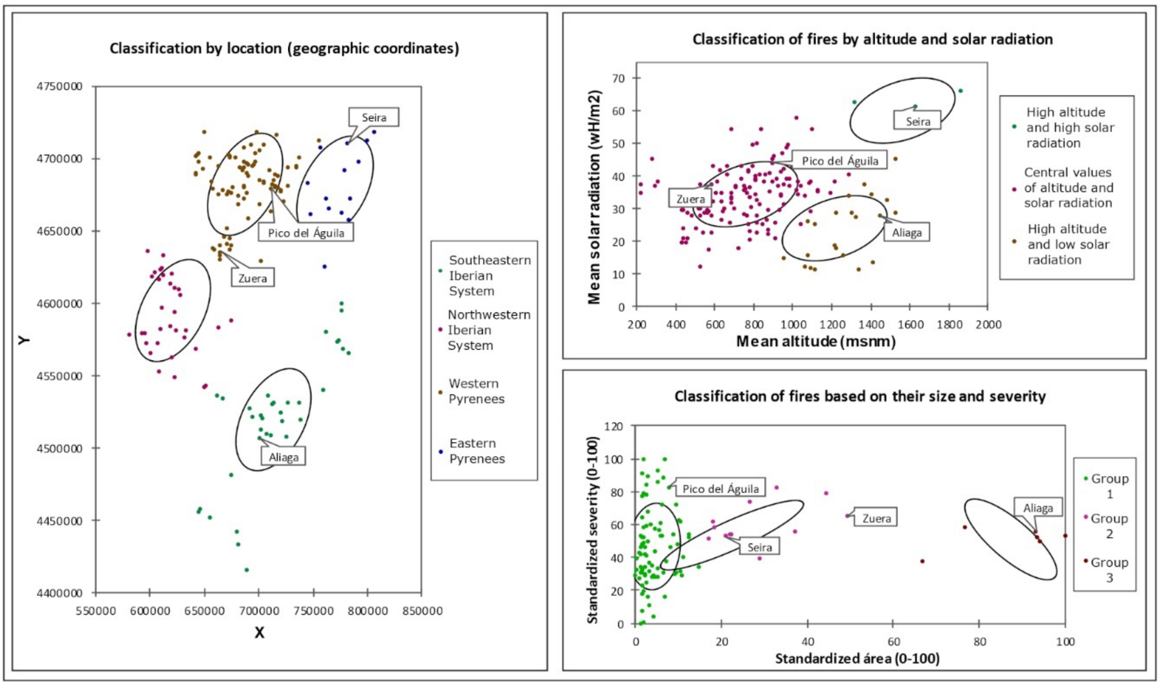

Figure 3. Graphical representation of fire distribution based on scenarios defined by pairs of characteristics: (i) geographic location (x, y coordinates); (ii) environmental factors related to solar radiation and altitude, and (iii) fire severity (size-severity); ellipses limit the groupings determined by GMM models, nominal labels identify the location of selected fires.

3.2.2. Digital processing and classification of Geosat-2 imagery

The GeoSAT-2 images underwent a radiometric correction process to convert the data to reflectance and eliminate atmospheric interferences. The physical model of radiative transfer 6S *(Second Simulation of a Satellite Signal in the Solar Spectrum*) (Vermote *et al*., 1997) was used to carry out these corrections. This process was executed using Python's Py6s module (Wilson, 2013).

A supervised digital classification was then performed on the corrected GeoSAT-2 images to identify the vegetation composition in the burned areas. The phenological component was incorporated using two images of different temporal moments (spring and autumn) from the years 2021-2023, combined in a multiband image. To avoid information redundancy, a principal component analysis (PCA) was performed, obtaining a reduced set of bands without significant loss of information.

The supervised digital classification process on the image resulting from the PCA began with the selection of representative pixels of each category by means of ROIs (Regions of Interest), defined from a visual analysis of orthophotos and false color satellite images, as well as field samples. After determining the representative pixels of each forest category, the spectral separability of the samples was evaluated using the divergence and *Jeffries-Matusita* (JM) distance methods to ensure correct differentiation. Once the spectral categories were defined, we assigned them pixels using the Maximum Likelihood (ML) method, based on the probability that a pixel belongs to a specific category.

$$g_i(x) = 1np(\omega_i) - {}^{1}/_{2}\, 1n|\textstyle\sum_i| - {}^{1}/_{2}\,(x - m_i)^{T\cdot} \textstyle\sum_i^{-1}(x - m_1) \qquad \text{(Eq. 1)}$$

Where i is the class; p are the n -dimensional data (where n is the number of bands); p(ω_i) is the probability that the class ω_i occurs in the image; |Σ |is the covariance matrix of the data in class ωi; $^{\Sigma i\text{-}1}$ is the inverse matrix; and m_i is the mean vector (Richards, 1999).

The reliability analysis was carried out through a verification process comparing reference points (ground-truth) with the classification values to obtain the Kappa coefficient that evaluates the quality of the product according to the thresholds of Landis and Koch (1977). Ground-truth data were obtained from field campaigns conducted during 2023 and 2024 using Leica Geosystems® (GNSS-Global Navigation Satellite System) global positioning equipment and high-resolution orthophotographs from the Plan Nacional de Observación del Territorio (PNOT). The total validation sample included 294 points, of which 60 were collected directly during field campaigns.

3.2.3. Obtaining the spatial distribution of LAI data by wildfire

LAI data were obtained from S2- L2A images using the SNAP *(Sentinel Applications Platform*) *Biophysical Processor*, which generated a comprehensive database of vegetation characteristics and associated canopy top reflectances (TOC: Top Of Canopy) of S2. The algorithm was then applied to each of the monthly S2 satellite images, resulting in a LAI product for each month of the years 2020-2023. To obtain a single value of the summer LAI per fire, a map algebra process was carried out to provide the average LAI of each pixel.

3.2.4. Obtaining multitemporal NVDI trends

The NDVI trend was obtained from Landsat image collections by calculating the linear adjustment coefficients *(scale, offset*) of this multispectral index at the pixel level. The regression equations between time (independent variable) and NDVI values at each pixel were calculated using the least squares method (Eq. 2). The slope or trend of the NDVI values was obtained from the equation (Eq. 3).

All this processing was developed on the *Google Earth Engine* platform. As part of the processing, masks were applied to reduce cloud interference, scale factors were adjusted, and a noise filter was used to keep NDVI values in the range of 0.15 to 0.9, thus avoiding outliers.

$$y = a + bx \qquad \text{(Eq. 2)}$$

$$b = \frac{\sum_{i=1}^{n}(x_1 - \bar{x})(y_1 - \bar{y})}{\sum_{i=1}^{n}(x_1 - \overline{x})^2}$$

$$a = \bar{y} - b\bar{x}\ \mathrm{b}$$

Where n is the number of observations x_1 and $y_1$are the values of the independent and dependent variables; $\bar{x}\ \bar{y}$ are the means of the variables (Mateos-Aparicio, 2011).

$$NDVI = scale\ \times\ time + intercept \qquad \text{(Eq. 3)}$$

3.2.5. Applied statistical methods

3.2.5.1. Contingency tables

Contingency tables are used to study changes in the composition and spatial distribution of plant formations. These tables record the correspondences between vegetation formations at two specific times: before the fire (columns) and after the fire (rows); where the diagonal indicates: (a) the number of pixels that maintain the same vegetation category (i.e., pixels recovered in the same location); and (b) the marginal values that document the displacement infringed by other categories and the expansion over them (i.e., *omission* and *commission*, respectively).

In this work, the frequencies were relativized according to the area of each fire. The classical metrics of accuracy and precision are adjusted to evaluate the relationships and conflicts between coverages by means of three indicators: *invasiveness* (I), *malleability* (M), calculated from the sum of the percentages corresponding to false positives and negatives, respectively; and *correspondence* (C), which measures only the coincidences considering the two moments. While the concept of *invasion* is related to the ability to occupy areas other than pre-fire zones, *malleability* here means the opposite of resistance. In this context, it refers to formations that undergo profound changes in their composition and show little ability to maintain their initial spatial distribution.

Additionally, *Chi-square* and *Fisher* tests were used to analyze the independence and degree of association between rows and columns, as well as *Goodman's and Kruskal's Gamma* coefficient. On the other hand, we applied *Kruskal-Wallis* and post-hoc tests using *Dunn'*s method with *Bonferroni* correction to analyze the distribution of LAI values by fire and regenerative trajectory.

3.2.5.2. Application of predictive modeling (RF)

The *Random Forest* (RF) machine learning algorithm (Cutler *et al.*, 2012) was used to develop a classification model that determined the extent to which various factors influenced the spatial distribution of current plant formations. The algorithm was implemented in R code using the *randomForest* package of Breiman *et al.* (2001). In this case, a database of approximately 10,000 records was used. The code performed 10 random samples, each with a sample size of 3,000 records (400 corresponding to each current forest formation and fire). In order to ensure the robustness of the prediction, this process was repeated 20 times.

Each implemented RF had 500 different trees, a commonly used parameter that is large enough to capture the variability of the data (Geron, 2019). In the model developed, the dependent variable was the vegetation that occupied the areas affected by fires, identified from the digital classification of GeoSAT-2 images. Predictors included fire severity, pre-existing vegetation, NDVI trend over 15 years post-fire, and landscape type where each fire occurred. The accuracy percentage of each model was calculated, as well as the final average of all models and the out-of- bag (OOB) misclassification rate. In addition, the average importance of each predictor variable as well as the *Partial Dependence Plots* (PDP) were obtained to show how they affected the response variable. The effects of the other variables in the model remained constant.

4. Results

4.1. Spatial distribution of colonizing vegetation formations

The digital classification of GeoSAT-2 images made it possible to identify the spatial distribution of the most representative vegetation formations that currently occupy the burned areas for each fire (Fig. 4-7). Table 1 shows the classification accuracy indicators which, in general terms, reach satisfactory levels *(Kappa* > 85%). The Seira fire was dominated by formations of *Pinus sylvestris* and *Quercus gr. cerrioides*, scrub communities dominated by *Buxus sempervirens* on the lower slopes, and subalpine pastures in the upper parts. In Pico del Águila there were small stands of *Pinus sylvestris*, *Quercus gr. cerrioides* and *Quercus ilex*, together with scrubs dominated by *Buxus sempervirens*, accompanied by *Genista scorpius* and *Quercus coccifera*. In the Zuera fire, the area was mostly occupied by *Pinus halepensis* and, to a lesser extent, by *Quercus ilex*, with sclerophyllous scrubs of *Genista scorpius* and *Quercus coccifera*. In Zuera, we found small stands of *Pinus halepensis* and *Quercus ilex*, with a predominance of *Genista scorpius* scrub, which in some sectors was accompanied by *Juniperus oxycedrus* woody scrub and in others by *Quercus coccifera.*

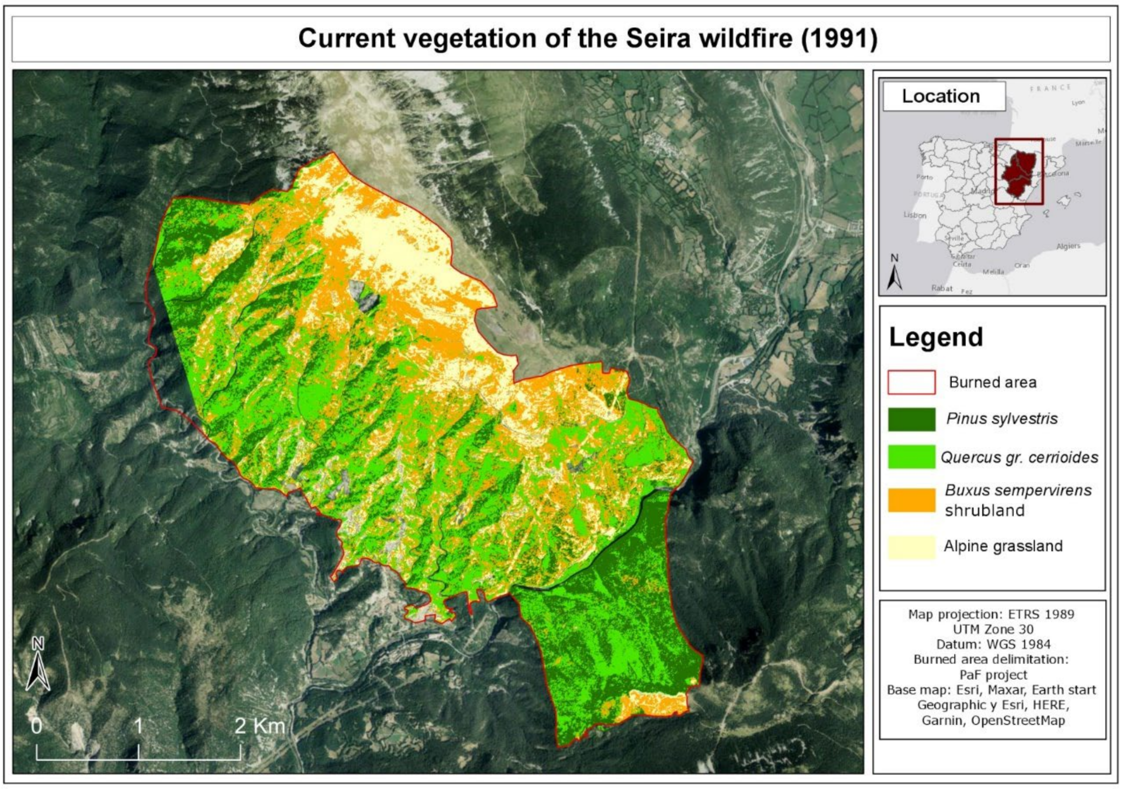

Figure 4. Current vegetation of the Seira fire.

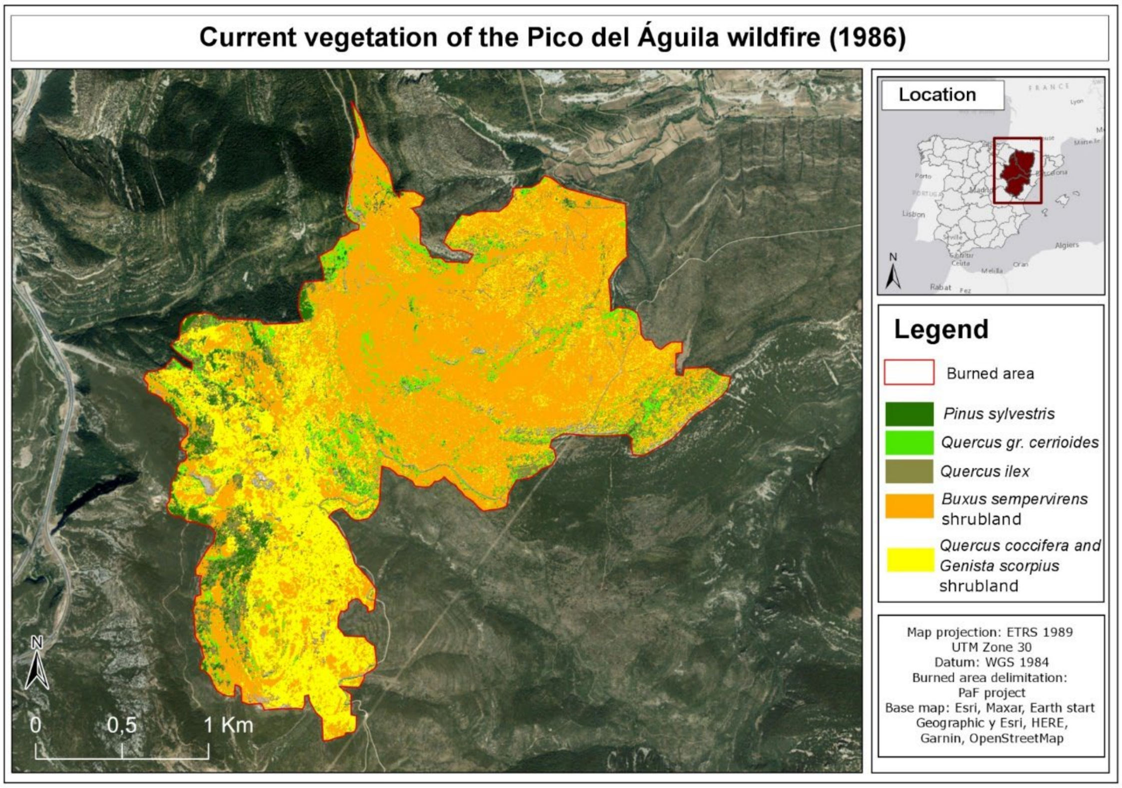

Figure 5. Current vegetation of the Pico del Águila fire.

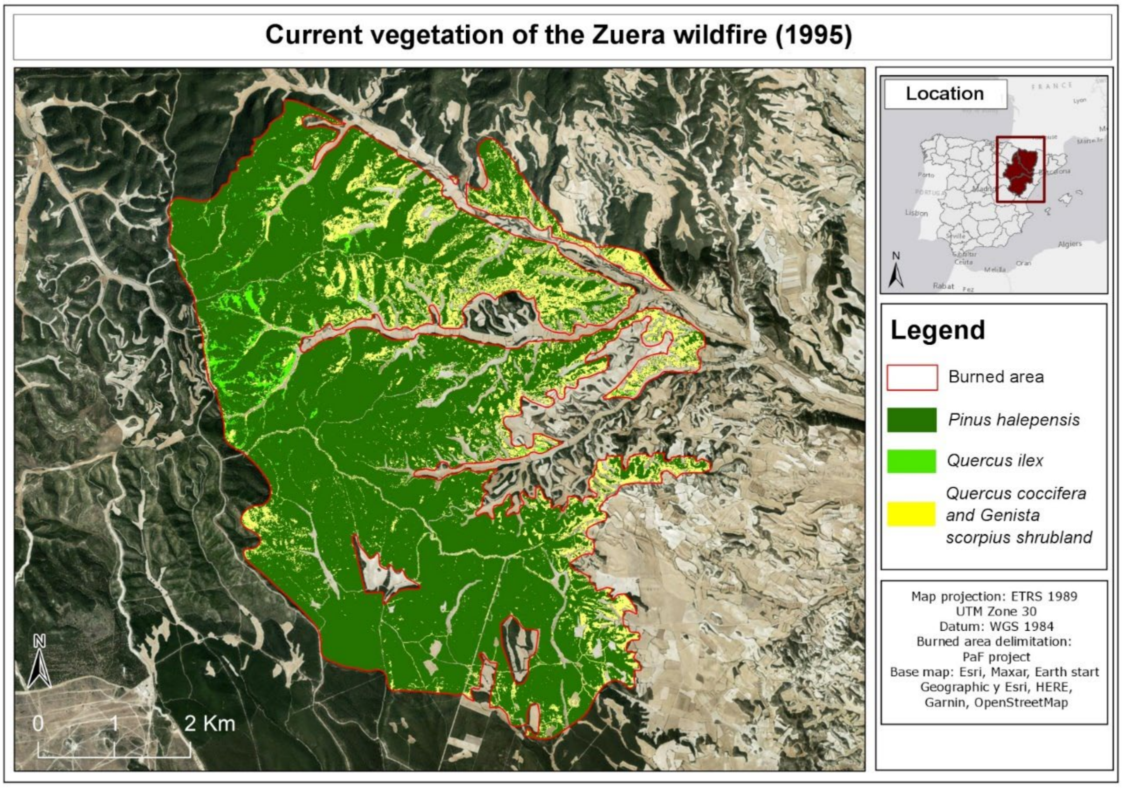

Figure 6. Current vegetation of the Zuera fire.

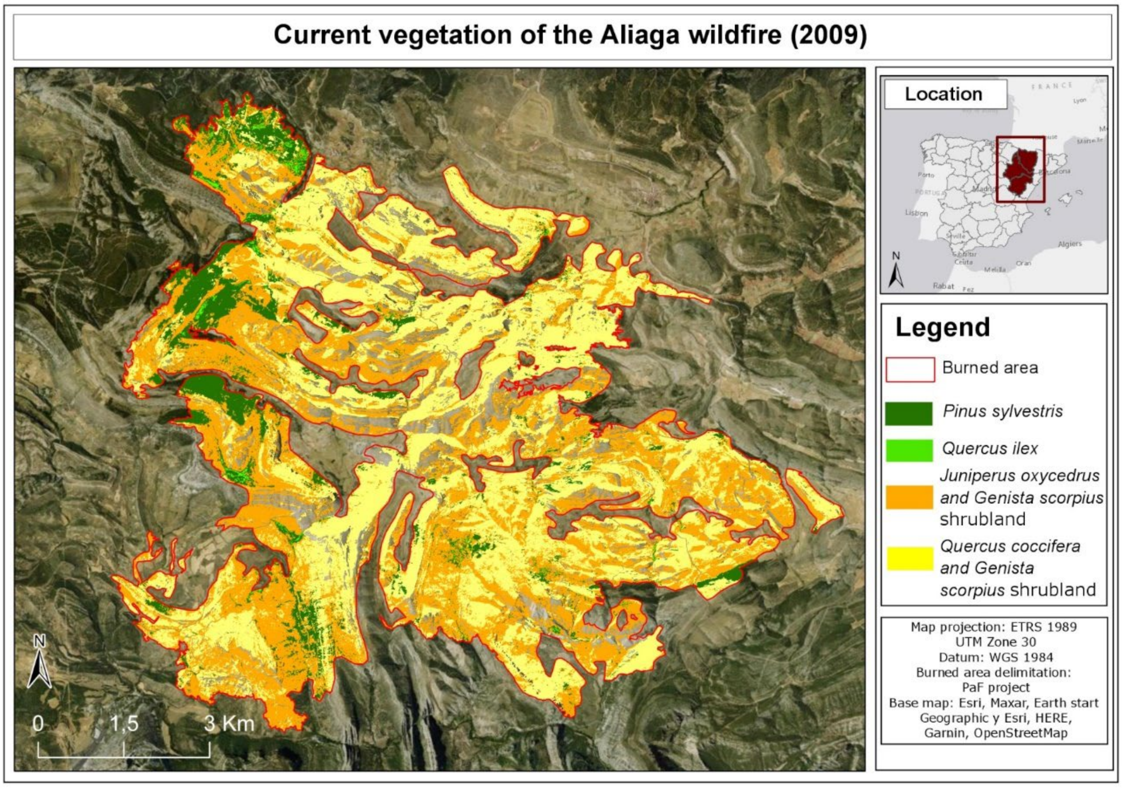

Figure 7. *Current vegetation of the Aliaga fire.*

Table 1. Results of the validation of the classification process using Geosat-2 images.

Fire	Ground-truth sample	Accuracy	Kappa Coeff.
Pico del Águila-1987	78	92.1%	0.89
Seira-1991	46	93.1%	0.86
Zuera-1995	42	90.4%	0.85
Aliaga-2008	128	94.5%	0.91

4.2. Relationships between pre- and post-fire vegetation formations

Table 2 shows the contingency matrices depicting the degree of agreement between vegetation types at two points in time (pre-fire and current) for the four fires. Prior to this analysis, it was necessary to (1) apply a homogenization process of the map key for each fire. It consisted of grouping the main shrub and subshrub species into two facies of scrubland: (MS) sub-Mediterranean scrub, dominated by *Buxus sempervirens* and to a lesser extent by other species such as *Echinospartum horridum*; (ME) sclerophyllous scrub, dominated by *Genista scorpius,* accompanied by other species such as *Quercus coccifera*; (2) generalize the current forest cover information by applying a mode filter. This procedure involved assigning the majority category of current vegetation to each 30m pixel (corresponding to the pre-fire Landsat classification); (3) analyze the consistency of the trajectories from a sample of representative unburned pixels (n = 2.600), evaluating the degree of coincidence between pre- and post-fire classifications. An average coincidence of 83% was obtained.

The observed *Chi-square* value (10.067) revealed significant dependence between the occupancy of vegetation formations before and after the fire *(p_value* < 0.05). However, specific differences were observed in each fire. In this sense, Seira and Pico del Aguila showed the strongest levels of association (Goodman's and Kruskal Gamma values = 0.17 and 0.10, respectively). For Zuera and Aliaga, the values were below 0.04. Although a high degree of similarity was observed in the Pico del Águila fire, there was a notable increase in sub-Mediterranean scrub to the detriment of pre-fire areas dominated by *Pinus sylvestris* and Quercus. In the Zuera fire, *Pinus halepensis* formations had displaced *Quercus ilex* and sclerophyllous scrub. The most notable changes were observed in Aliaga because the current formations differ greatly from the original ones. Scrublands now occupy areas that were previously dominated by *Pinus sylvestris* and *Quercus ilex*.

Table 2. Contingency matrices between pre-fire and current vegetation due to fire.

	Current vegetation	Previous vegetation (pre-fire)				
		Pinus sylvestris	*Q. gr. cerrioides*	*Quercus ilex*	*MS_Bs**	*ME_Gs**
Seira	*Pinus sylvestris*	**11.40**	8.13	-	1.73	-
	Q. gr. cerrioides	8.09	**18.35**	-	7.80	-
	*MS_Bs**	4.69	9.77	-	**30.00**	-
Pico del Águila	*Pinus sylvestris*	**2.42**	0.18	0.00	0.00	0.00
	Q. gr. cerrioides	1.84	**0.45**	0.00	4.63	0.00
	Quercus ilex	3.80	0.00	**0.96**	2.52	0.11
	MS_Bs*	14.43	1.81	4.39	**60.60**	0.00
	*ME_Gs**	0.04	0.04	0.04	0.00	**1.58**
Zuera	*Pinus halepensis*	**52.75**	-	22.44	-	10.19
	Quercus ilex	1.01	-	**0.30**	-	0.24
	*ME_Gs**	4.35	-	2.71	-	**6.01**
Aliaga	*Pinus sylvestris*	**9.35**	-	0.00	-	0.00
	Quercus ilex	0.33	-	**0.39**	-	0.30
	*ME_Gs**	31.97	-	17.01	-	**40.58**

(*) *MS_Gs (Genista scorpius submediterranean scrub); ME_Gs (Genista scorpius sclerophyllous scrub); MS_Bs (Buxus sempervirens submediterranean scrub).*

Considering the representative indicators of fire-induced ecological stress in the vegetation composition of the fires analyzed through residues (Fig. 8), *Pinus sylvestris* formations demonstrated high relative malleability (i.e., they underwent significant changes in composition and showed limited ability to maintain their initial state). These formations also exhibited low invasive capacity (i.e., limited ability to occupy areas other than those they were in before the fire). Moderate *malleability* values were only recorded in the case of the Seira fire, reflecting the higher level of *correspondence* of this formation in these environments.

In the case of *Quercus gr. cerrioides,* present in the Seria and Pico del Aguila fires, the values were notably disparate. While in Pico del Aguila this formation showed a low level of *correspondence*, in Seira it reached approximately 30%. On the other hand, holm oak groves were recorded, although with little relevance, in three of the four fires. These groves appeared to be very malleable formations, especially in Aliaga and Zuera.

Pinus halepensis forests were characterized by their low malleability and remarkable invasiveness. Finally, shrub formations showed very variable behavior depending on the area affected by the fires. These formations stood out for their particularly invasive character in Aliaga, their high *correspondence* in Pico del Águila and Seira, as well as their high *malleability* in Zuera.

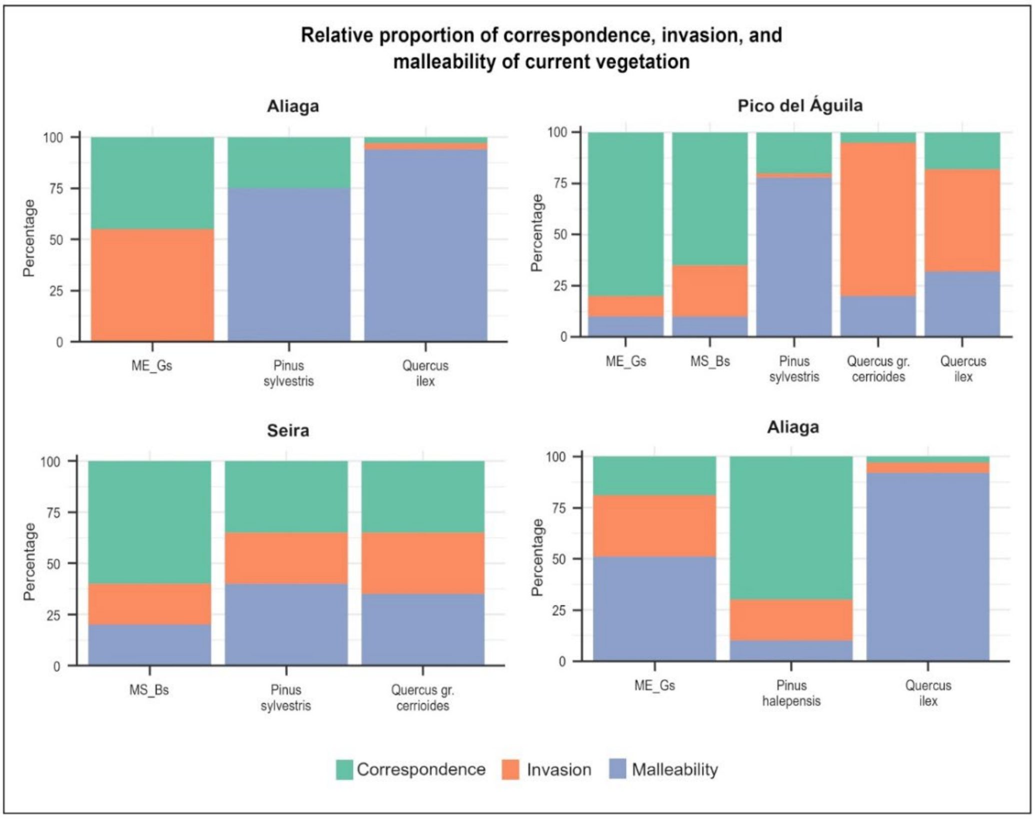

Figure 8. Relative proportion of correspondence, invasion, and malleability of current vegetation.

4.3. LAI levels based on vegetation transitions (pre and post fire)

In relation to the spatial composite of LAI values (Fig. 9), statistically significant differences were found between fires *(p-value* <0.05). The highest values were recorded in Seira, where scrubs of regenerated *Quercus gr. cerrioides , Pinus sylvestris,* and *Buxus sempervirens* predominate. As shown in Table 3, the Zuera and, especially, the Aliaga fires recorded the lowest LAI values. In the latter case, this was due to the abundance of small bushes and sparse woodland.

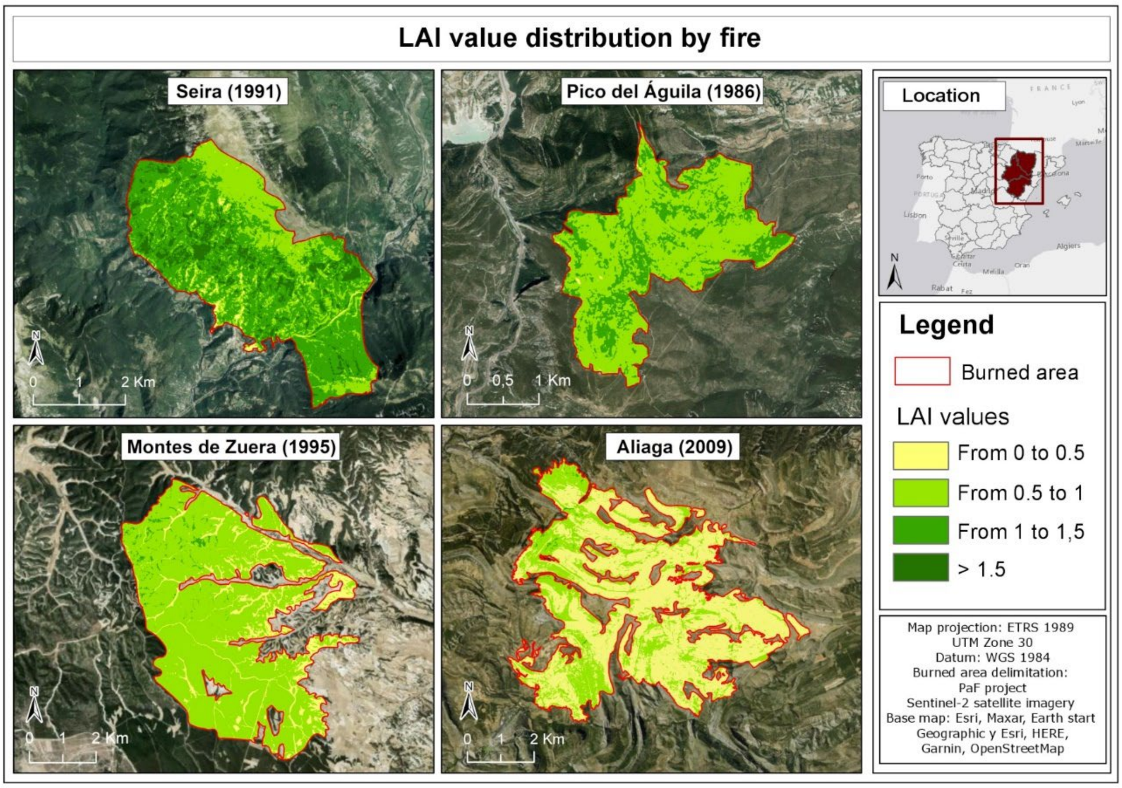

Figure 9. LAI distribution in each fire.

Table 3. Descriptive statistics of LAI values in each fire.

Fire	Mean	Mode	Standard deviation	Maximum	Minimum
Seira	1.18	1.33	0.27	2.1	0.2
Pico del Águila	0.92	0.85	0.12	1.3	0.3
Zuera	0.72	0.72	0.19	1.6	0.0
Aliaga	0.48	0.42	0.13	1.1	0.0

Analyzing transitions or changes between plant formations and their relationship with LAI enabled the integration of two dimensions of regeneration. Significant differences were observed between transitions (Kruskal-Wallis *p-value* < 0.05). In general terms, as shown in Table 4, LAI values were higher in burned areas that had evolved into tree communities (moderate-high and high LAI groups), especially in the case of *quejigares (Quercus faginea forests).* In contrast, transitions from arboreal to shrubland formations recorded the lowest LAI values.

However, *Genista scorpius* sclerophyll shrub formations showed significant differences depending on whether they originated from *Genista scorpius* or from *Pinus halepensis*, reaching higher LAI values in the latter case *(p-value* <0.05). In the case of sub-Mediterranean *Buxus sempervirens* shrublands, LAI values increased depending on whether they were the result of their own recovery or if they originated from fires on *Quercus gr. cerrioides* formations. *Quercus ilex* also showed some sensitivity to its provenance. Finally, *Pinus sylvestris* and *Quercus* gr. *cerrioides* showed differences, although not significant, depending on their origin.

Table 4. Main pairwise multiple comparisons using Dunn's test. L: low LAI values; ML: moderate-low LAI values; M: moderate values; MH: moderate-high LAI values; H: high LAI values. Combinations belonging to several groups did not show significant evidence for separation (i.e., they were on the borderline of the two groups)

	Frequency	Average of ranges	LAI Groups				
ME_Gs *from* ME_Gs	970	1398	L				
ME_Gs *from Ph*	226	2238		ML			
ME_Gs *from Ps*	454	1246	L				
ME_Gs *from Qi*	161	1534	L				
MS_Bs *from* MS_Bs	1005	3455			M		
MS_Bs *from Ps*	187	4009			M	MH	
MS_Bs *from Q gr. c*	136	4754				MH	H
Ph from ME_Gs	65	2691		ML	M		
Ph from Ph	400	3207			M		
Ps from Ps	782	3582			M		
Q gr. c from Ps	369	5337					H
Q gr. c from Q gr. c	477	5278					H
Qi from ME_Gs	157	3319			M		
Qi from Ps	280	3682			M		
Qi from Qi	447	2659		ML			

4.4. NDVI regenerative trends

The NDVI trend during the 15 years after the fires evidenced differences in the regenerative dynamics of the studied areas (Table 5). Pico del Águila and Zuera had the highest average trends and the lowest variability. Seira, on the other hand, presented an intermediate average value accompanied by low variability, which reflects a moderate and uniform trajectory of plant recovery. In contrast, Aliaga stood out for its less pronounced and dispersed regenerative tendency. It also exhibited negative tendencies. Variations between plant formations were also recorded. Among them, the high tendency of *P. halepensis* in Zuera and the high generalized tendencies of *Quercus gr. cerrioides* stood out.

Table 5. Descriptive statistics of NDVI trend during the first 15 years after each fire. The values are presented multiplied by 100 to allow a more detailed analysis, since the original ones were very low.

Fire	Mean	Mode	Standard deviation	Maximum	Minimum
Seira	1.01	0.74	0.21	2.20	0.01
Pico del Águila	1.53	1.54	0.24	2.61	0.02
Zuera	1.27	2.20	0.22	2.40	0.01
Aliaga	0.89	0.41	0.39	1.91	-0.26

4.5. Factors responsible for the spatial distribution of plant formations

Regarding the prediction of the plant formations colonizing the burned areas, the RF models applied to determine the role played by the set of predictors offered acceptable accuracy values (average = 79%), with an OOB error rate of 21%. The most significant variable was pre-existing vegetation, with a *Mean Decrease Gini* (MDG) value of ~ 600. The remaining variables had a smaller impact on the model's decisions (MDG < 300), with landscape being the least important. However, the severity and trend quantitative variables operated differently depending on the type of plant formation.

Figure 10 shows how the probabilities of belonging to a category changed as severity and trend did, while holding constant or averaging the effects of the other variables. In this sense, in the case of severity (Fig. 10A), while in shrub formations the probabilities of belonging to a category increased as severity did, in the case of *P. sylvestris* formations, the model prediction operated in the opposite direction and in a very pronounced way (i.e., it decreased as severity increased). Likewise, quercineae and, especially, *P. halepensis,* did not show a significant relationship.

With regard to the trend (Fig. 10B), the influence on prediction was less pronounced. The most significant cases corresponded to ME, which showed an inverse relationship, and to gall oak and Ps where there was a certain increase in the probability with high trends (>0.01). In the case of holm oak and MSB, the prediction in the models was not sensitive to the regenerative trend through the multitemporal analysis of the post-fire NDVI.

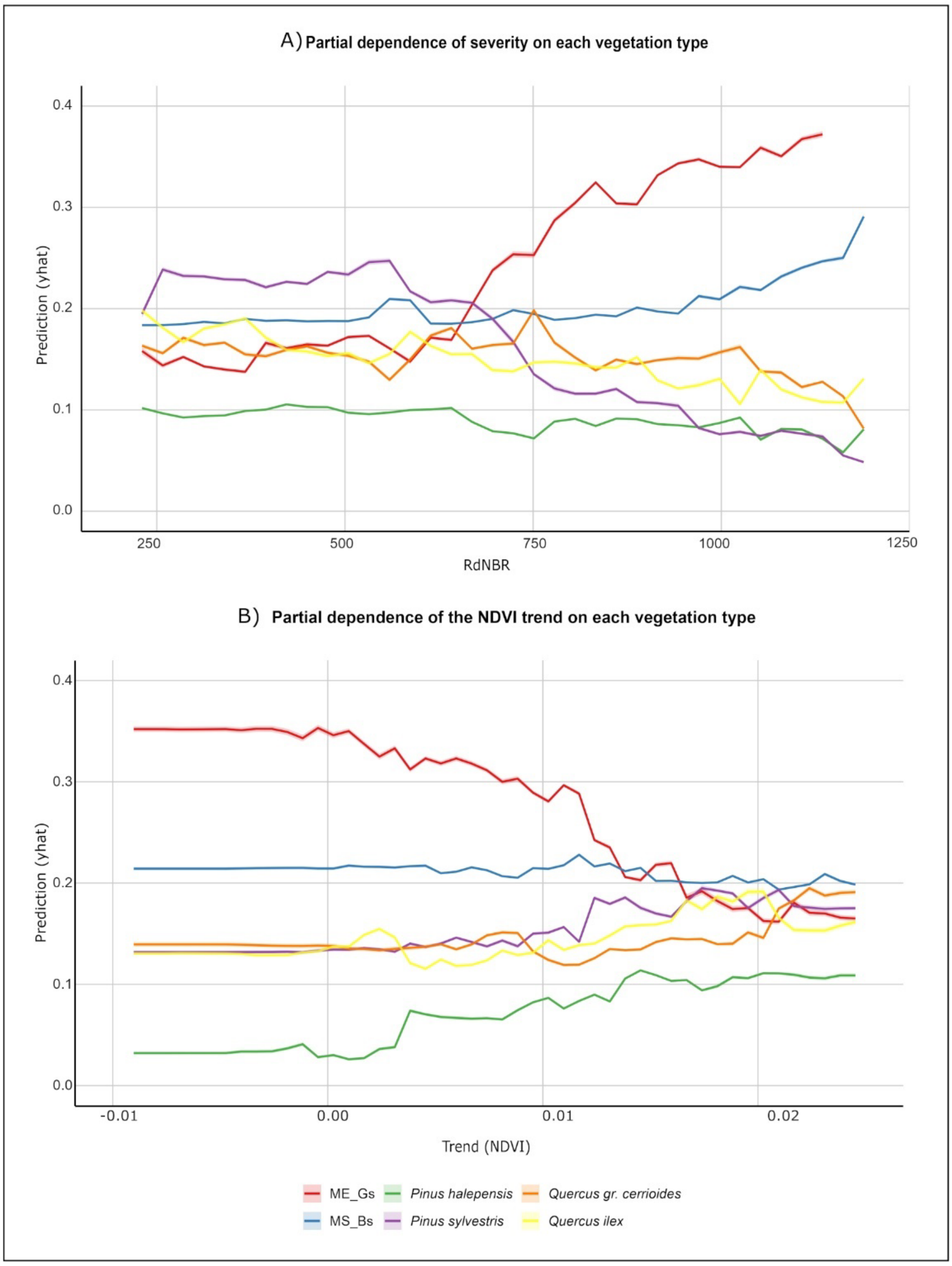

Figure 10. Partial dependence of fire severity and trend (NDVI) on each pre-existing vegetation type.

5. Discussion

The results of this study describe the levels of plant regeneration in different landscapes in Aragon affected by fire, selected to cover the diversity of post-fire scenarios across the region. It integrates two key dimensions of the recovery process: the type of colonizing plant formation in relation to the pre-existing one, and its impact on the levels of Leaf Area Index (LAI), which was used as a proxy of the intensity of eco-physiological functions. The two dimensions were addressed by combining two methodological approaches: (i) contingency tables derived from diachronic comparisons of the dominant vegetation type at the pixel level (before and after fire), and (ii) *Random Forest* (RF) based predictive models. Four fires were selected as a representative sample to reflect the diversity of forest landscapes in Aragon affected by fire.

5.1. Plant formations and distribution of LAI values

Supervised digital classification processes using high spatial resolution images (GeoSAT-2) allowed us to know the distribution of current vegetation and to analyze the changes in relation to the previous distribution. In general terms, the plant formations found in the burned areas are similar to the pre-existing ones. This is consistent with a large number of studies on similar communities using experimental plots (Lloret *et al.*, 2003; Pérez-Cabello, 2002). However, differential behaviors were observed in relation to some species and specific locations.

The areas with less correspondence between plant species were located in the Aliaga fire. This fire is representative of the *Macizos Ibéricos Calcáreos* belonging to the potential series of holm oak groves. Currently, the burned area is mainly occupied by Mediterranean subshrub shrublands. Pre-fire areas dominated by *Pinus sylvestris* are now only recognized in small stands. The low regeneration of these pine forests in Aliaga could be attributed to the lower regenerative efficiency of this species in the face of severe fires, as pointed out by Martín-Alcón and Coll (2016). These pine forests do not have serotinous properties, so after a high severity fire, much of the canopy seed bank may have died, hindering recovery processes. However, there were specific locations (Seira fire) in which the spatial correspondence before and after the fire was significant. This is a result of the greater effectiveness of *Pinus sylvestris* in this type of landscape *(Macizos Pirenaicos Calcáreos de Alta Montaña*, belonging to the series of the *pinares albares*). This difference may also be related to the severity of the fire. Seira presented moderate average values and many areas of low severity. Alternatively, it might be related to the amount of time elapsed since the fire (~ 30 years compared to 14 years in Aliaga). This pattern is in agreement with the results documented by Calama *et al.* (2017), Retana *et al.* (2012) and Maren *et al.* (2023).

The pine forests, specifically those belonging to the *P. halepensis* species, were dominant in the Zuera fire and showed excellent levels of recovery, occupying much of the area burned in 1995. This high resilience is related to its serotinous properties, an adaptive strategy that keeps seeds stored in closed cones that only open in response to stimuli such as heat from a forest fire (Habrouk *et al*., 1999). In the long term, the success of *Pinus halepensis* has even allowed it to invade areas dominated by shrub species with a regenerative strategy based on regrowth such as *Quercus ilex* and *Q. coccifera*. These results are consistent with those obtained in other areas of the Mediterranean region, as reported by Moya *et al.* (2019), Elvira *et al*. (2021), and Kazanis *et al.* (2024).

A high correspondence was identified in the plant formations dominated by *Buxus sempervirens*, *Quercus coccifera*, and *Genista scorpius.* However, they also showed an important invasive potential as they constituted the degraded series of tree formations affected by fire. Resprouting shrubs, such as boxwoods, have a high ability to generate new shoots immediately after fire due to reduced competition for resources (Keeley, 1981). *Quercus gr. cerrioides* and *Quercus ilex* exhibited high malleability. However, an important invasive ability was also identified due to their active regenerative strategy in pine forest areas. These results are in line with other studies, such as those reported by Galiano *et al.* (2013).

In summary, the indicators of invasiveness and malleability revealed the different response of plant formations. On the one hand, *Pinus sylvestris* showed high malleability and low invasiveness in all fires. However, this pattern was less pronounced in the Seira fire. Quercineae also showed high malleability values, but with a high colonizing ability in areas different from those they occupied before the fire. As for the pine forests of *P. halepensis* and the sub-Mediterranean and sclerophyllous shrublands, the malleability was found to be low, with a very high invasive ability.

In relation to LAI values, the type of vegetation formation is key to explain its distribution. However, the kind of transition between pre- and post-fire vegetation formations also determines differences within the same formation. In this sense, certain patterns were identified in the current distribution of LAI based on the characteristics of the transition. For example, the higher LAI values observed in sclerophyllous shrublands dominated by Genista scorpius that originate from Pinus halepensis stands suggest that post-fire regeneration is strongly influenced by the ecophysiological legacy of the pre-fire pine forest. This legacy confers an initial competitive advantage to colonizing species by enhancing resource acquisition and facilitating the reactivation of photosynthetic activity after fire (through a greater capacity to capture light, water, and nutrients, and to regulate key physiological processes such as photosynthesis and transpiration). Such a pattern may represent a case of partial autosuccession, in which post-fire communities retain functional attributes from the preceding ecosystem, leading to more efficient and stable recovery trajectories.

A similar trend is found in post-fire shrublands dominated by Buxus sempervirens, where LAI values are significantly higher when derived from Pinus sylvestris or, particularly, Quercus gr. cerrioides forests. This finding indicates that the pre-fire vegetation type not only shapes the subsequent floristic composition but also influences photosynthetic efficiency and structural recovery potential—likely mediated by the persistence of seed banks, belowground organs, or functional traits inherited from the original forest.

As emphasized by Woodgate *et al.* (2024), combining vegetation type (composition) with quantitative indicators such as LAI provides a more accurate assessment of the degree of autosuccession, the intensity of photosynthetic activity, and the efficiency of light use throughout the regeneration process. These results highlight that post-fire shrubland ecosystems retain a form of ecological memory that modulates their successional trajectories after disturbance. This memory is expressed through functional traits governing resource-use efficiency and structural recovery, and represents a key mechanism underpinning the resilience and adaptive capacity of Mediterranean ecosystems under changing climatic conditions and increasingly altered fire regimes.

These findings regarding LAI and the ecological legacy of pre-fire communities are further supported by predictive modeling using RF, which allowed us to determine the weight of different factors on the spatial distribution of current species. In this sense, the reproductive strategy of each species plays a fundamental role in post-fire regeneration, as widely reported in the scientific literature (Alloza *et al.*, 2006; Parra and Moreno, 2018; Pausas *et al.*, 2004; Santana *et al.*, 2012) and reinforced here using remote sensing data.

Moreover, the importance of factors such as severity and regenerative tendency, both analyzed using spectral indices, is also critical in predictive modeling, as described in other works (Chen *et al.*, 2011; Francos *et al.*, 2018; Shvetsov *et al.*, 2019). In the case of trends, although the NDVI may be limited by soil influences in areas with sparse vegetation cover or phenological influences on data readings (Pettorelli *et al.*, 2005), it was a variable with significant predictive value. NDVI´s role may reflect cumulative processes that influence the system's dynamics and vary depending on plant formations, which exhibit different regenerative behaviors over time. Finally, severity modulated the regeneration of plant formations in a differential manner: in areas of high severity, the probability of colonization by shrublands increased, whereas the regeneration of non-serotinous germinating species, such as *P. sylvestris*, was reduced.

5.2. Limitations and difficulties arising from the use of multisensor products

GeoSAT-2, Landsat 5-8 and Sentinel-2 data were used in this study, which involved working with different spatial, spectral, and temporal resolutions. GeoSAT-2 images were used to carry out a digital classification process in order to identify the communities currently occupying the burned areas. These classification processes were based on the spectral behavior of the image pixels, so the number of spectral bands can influence the results. GeoSAT-2 images present only three bands in the visible and one in the near infrared, resulting in a limited reflectance spectrum, unlike other images such as Landsat that provide spectral information over a wider range.

To improve image classification and reduce the influence of low spectral resolution, two satellite images from different time points were used. This made it possible to introduce the phenological perspective, allowing a better identification of certain forest communities. This method, together with the small pixel size, enabled accurate and high quality identification. However, these images are only available from 2021 to 2023. This makes it impossible to identify plant formations using high spatial resolution in time periods prior to the fires.

For the identification of the pre-existing formations, we used products derived from Landsat images with a spatial resolution of 30 m. In order to establish adequate comparisons between pre-existing and present communities, it was necessary to reduce the spatial resolution of GeoSAT-2 to the Landsat level, using mode filtering. This transformation introduced some uncertainty in the comparison between pre-existing and current formations. However, an analysis in control zones not disturbed by fire (invariant zones), allowed us to verify the degree of multi-temporal correspondence of the categories, resulting in an average coincidence level of 83%. This implied an uncertainty of 17% in the results obtained from the comparison between pre- and post-fire conditions, which made it possible to detect the most outstanding changes in the communities as shown in the results. The lack of correspondence in "vegetation invariant" zones can be attributed to the uncertainties inherent to the classification process, and to the bias in generalizing the current vegetation with a centrality parameter (mode).

6. Conclusions

In general terms, and based on the results obtained in this study, it can be concluded that plant regeneration is more significant in areas previously dominated by species with active reproductive strategies (resprouting or serotiny). However, greater regeneration difficulties are observed in areas characterized by species with passive reproductive strategies, such as Pinus sylvestris. In addition to the pre-existing vegetation type, the results underline the relevance of considering the successional trajectory or the change in the composition of the dominant vegetation to characterize the spatial distribution of leaf area index (LAI) values. This index is used as a proxy of the ecophysiological functions of the regenerated vegetation. Random Forest (RF) modeling reaffirms the influence of pre-existing vegetation, particularly in its interaction with fire severity, regenerative tendency, and landscape context. To strengthen the robustness of the study, we propose including other plant formations and incorporating new variables (e.g., climatic parameters, hydrological-forestry treatments), in order to establish more precise relationships between environmental conditions and post-fire ecosystem responses.

The development of integrative models that consider both the composition of regenerated species and their influence on ecophysiological processes could improve forest management strategies.

This would enable the implementation of more efficient conservation techniques, thereby optimizing biodiversity restoration and preservation efforts in the context of recurring forest fires.

Acknowledgments

This work is part of the R+D+i project "Dynamic analysis of the resilience of Fire Affected Forest Landscapes (PaF) using multisensor spectral indicators", funded by the Ministry of Science, Innovation and Universities of the Government of Spain (projects CGL2016-80783-R, 2016 and PID2020-118886RB-I00, 2020). This project has facilitated access to Geosat-2 high spatial resolution images, which are essential for the development of the present study (General Action Protocol between the IGN/CNIG and CDTI. Copyright © GEOSAT. We would also like to thank the Government of Aragón for funding the doctoral grant awarded to Pedro Martín Ortiz (call for applications 2024-2028).

References

Alloza, J.A., Baeza, M. J., de la Riva, J.R., Duguy, B., Echeverría, M.T., Ibarra, P., Llovet, J., Pérez-Cabello, F., Rovira, P., Vallejo, R., 2006. A model to evaluate the ecological vulnerability to forest fires in Mediterranean ecosystems. Viegas, D.X. (ed.) *Actas de la 5ª Conferencia Internacional sobre Investigación de Incendios Forestales*. Ámsterdam: Elsevier, 12.

Ancira-Sánchez, L., Treviño, E. J., 2015. Utilización de imágenes de satélite en el manejo forestal del noreste de México. *Madera y Bosques, 21*(1), 77-91.

Bassett, M., Leonard, S.W.J., Chia, E.K., Clarke, M.F., Bennett, A.F., 2017. Interacting effects of fire severity, time since fire and topography on vegetation structure after wildfire. *For. Ecol. Manage. 396*, 26-34. https://doi.org/10.1016/j.foreco.2017.04.006

Bodí, M.B., Cerdá A., Mataix-Solera, J., Doerr, S., 2012. Efectos de los incendios forestales en la vegetación y el suelo en la cuenca mediterránea: Revisión bibliográfica. *Boletín de la Asociación de Geógrafos Españoles, 58*, 35-55.

Breiman, L. 2001. Random forests. *Machine Learning, 45*(1), 5-32. https://doi.org/10.1023/A:1010933404324/METRICS

Calama, R., Manso, R., Lucas-Borja, M. E., Espelta, J. M., Piqué, M., Bravo, F., del Peso, C., Pardos, M. 2017. Natural regeneration in Iberian pines: A review of dynamic processes and proposals for management. *Forest Systems, 26*(2), eR02S. https://doi.org/10.5424/fs/2017262-11255

Cerdà, A., Robichaud, P.R., 2009. *Fire Effects on Soils and Restoration Strategies* (1st ed.). CRC Press. https://doi.org/10.1201/9781439843338

Chaves, M.E.D., Picoli, M.C.A., Sanches, I.D. 2020. Recent Applications of Landsat 8/OLI and Sentinel-2/MSI for Land Use and Land Cover Mapping: A Systematic Review. *Remote Sensing, 12*(18), 3062. https://doi.org/10.3390/RS12183062

Chen, J. M., Black, T. A., 1992. Defining leaf area index for non-flat leaves. *Plant, Cell and Environment*, *15*(4), 421-429. https://doi.org/10.1111/J.1365-3040.1992.TB00992.X

Chen, X., Vogelmann, J.E., Rollins, M., Ohlen, D., Key, C.H., Yang, L., Huang, C., Shi, H., 2011. Detecting post-fire burn severity and vegetation recovery using multitemporal remote sensing spectral indices and field-collected composite burn index data in a ponderosa pine forest. *International Journal of Remote Sensing*, *32*(23), 7905-7927. https://doi.org/10.1080/01431161.2010.524678

Choudhury, M.A.M., Marcheggiani, E., Despini, F., Costanzini, S., Rossi, P., Galli, A., Teggi, S., 2020. Urban Tree Species Identification and Carbon Stock Mapping for Urban Green Planning and Management. *Forests 2020, 11*, 1226. https://doi.org/10.3390/F11111226

Chu, T., Guo, X., Takeda, K., 2017. Effects of burn severity and environmental conditions on post-fire regeneration in Siberian Larch forest. *Forests 8*, 1-27. https://doi.org/10.3390/f8030076

Cutler, A., Cutler, D.R., Stevens, J.R., 2012. Ensemble Machine Learning. *Ensemble Machine Learning*, *January*. https://doi.org/10.1007/978-1-4419-9326-7

Elvira, N.J., Lloret, F., Jaime, L., Margalef-Marrase, J., Pérez Navarro, M.Á., Batllori, E., 2021. Species climatic niche explains post-fire regeneration of Aleppo pine (Pinus halepensis Mill.) under compounded effects of fire and drought in east Spain. *Sci. Total Environ. 798*, 149308. https://doi.org/10.1016/j.scitotenv. 2021.149308

Francos, M., Pereira, P., Mataix-Solera, J., Arcenegui, V., Alcañiz, M., Úbeda, X., 2018. How clear-cutting affects fire severity and soil properties in a Mediterranean ecosystem. *Journal of Environmental Management, 206*, 625-632. https://doi.org/10.1016/j.jenvman.2017.11.011

Galiano, L., Martínez-Vilalta, J., Eugenio, M., Granzow-de la Cerda, Í., Lloret, F., 2013. Seed- ling emergence and growth of quercus spp. following severe drought effects on a Pinus sylvestris canopy. *J. Veg. Sci. 24* (3). https://doi.org/10.1111/j.1654-1103. 2012.01485.x

Géron, A. 2019. Hands-on machine learning with Scikit-Learn, Keras, and TensorFlow (2nd ed.). O'Reilly Media.

Gitas, Z., Katagis, T., Toukiloglou, P., 2012. Burned area mapping and post-fire monitoring of a Mediterranean forest using NDVI time-series of low resolution imagery and the BFAST method / Mapeamento de área queimada e monitoramento pós-fogo de floresta na região Mediterrânea a partir de série tempor. *Revista Ambiência*, *8*(4), 461-470. https://doi.org/10.5777/ambiencia.2012.04.02

Grandes dominios de paisaje (ATLAS DE ARAGÓN - ICEARAGON). (n.d.). Retrieved November 11, 2024, from https://idearagon.aragon.es/atlas/Aragon/info/paisaje/grandes-dominios-de-paisaje/grandes-dominios-de-paisaje

Griffiths, P., Kuemmerle, T., Baumann, M., Radeloff, V.C., Abrudan, I. V., Lieskovsky, J., Munteanu, C., Ostapowicz, K., Hostert, P., 2014. Forest disturbances, forest recovery, and changes in forest types across the carpathian ecoregion from 1985 to 2010 based on Landsat image composites. *Remote Sensing of Environmen*t 151, 72-88. https://doi.org/10.1016/j.rse.2013.04.022

Gorelick, N., Hancher, M., Dixon, M., Ilyushchenko, S., Thau, D., Moore, R. 2017. Google Earth Engine: Planetary-scale geospatial analysis for everyone. *Remote Sensing of Environment*, *202*, 18-27. https://doi.org/10.1016/j.rse.2017.06.031

Habrouk, A., Retana, J., Espelta, J.M., 1999. Role of heat tolerance and cone protection of seeds in the response of three pine species to wildfires. *Plant Ecology, 145*, 91-99. https://doi.org/10.1023/A:1009851614885

Henry, M.C., Hope A. S., 1998. Monitoring post-burn recovery of chaparral vegetation in southern California using multi-temporal satellite data. *International Journal of Remote Sensing, 19*, 3097-3107. https://doi.org/10.1080/014311698214208

Instituto Geográfico Nacional., 2021. Cobertura Nacional VHR 2021-22–Documento explicativo de la cobertura en España con productos GeoSAT-2.

Iranzo Cubel, C., Acosta-Ruiz, A., Montorio Llovería, R., Hoffren, R., Pérez-Cabello, F., 2023. Evaluación de la maleabilidad de los paisajes forestales afectados por el fuego en Aragón. *Geografía: Cambios, Retos y Adaptación. XXVIII Congreso de La Asociación Española de Geografía. AGE y Universidad de La Rioja*, 165-174. https://doi.org/10.21138/cg/2023.lc

Jiménez, A., Pérez-Cabello, F., Montorio, R., 2016. Niveles de LAI/fPAR en superficies afectadas por incendios forestales en Aragón. Análisis mediante el producto MCD15A2 DE MODIS. *Pirineos*, *171*. http://dx.doi.org/10.3989/Pirineos.2016.171003

Juola, J., Hovi, A., Rautiainen, M., 2024. Comparison of contemporaneous Sentinel-2 and EnMAP data for vegetation index-based estimation of leaf area index and canopy closure of a boreal forest. *European Journal of Remote Sensing*, *57*(1). https://doi.org/10.1080/22797254.2024.2432975

Karavani, A., Boer, M.M., Baudena, M., Colinas, C., Díaz-Sierra, R., Pemán, J., de Luis, M., Enríquez-de-Salamanca, Á., Resco de Dios, V., 2018. Fire-induced deforestation in drought-prone Mediterranean forests: drivers and unknowns from leaves to communities. *Ecological Monographs*, *88*(2), 141-169. https://doi.org/10.1002/ecm.1285

Kazanis, D., Spatharis, S., Kokkoris, G.D., Dimitrakopoulos, P.G., Arianoutsou, M., 2024. Drivers of Pinus halepensis Plant Community Structure across a Post-Fire Chronosequence. *Fire 7.* https://doi.org/10.3390/fire7090331

Keeley, J.E., 1981. Reproductive cycles and fire regimes. *General Technical Report*, 231-277.

Keeley, J.E., 2012. Fire in Mediterranean climate ecosystems-A comparative overview. *Israel Journal of Ecology and Evolution*, *58*(2-3), 123-135. https://doi.org/10.1560/IJEE.58.2-3.123

Keeley, J.E., Fotheringham, C.J., Baer-Keeley, M., 2005. Factors affecting plant diversity during post-fire recovery and succession of mediterranean-climate shrublands in California, USA. *Diversity and Distributions*, *11*(6), 525-537. https://doi.org/10.1111/j.1366-9516.2005.00200.x

Korhonen, L., Hadi, Packalen, P., Rautiainen, M., 2017. Comparison of Sentinel-2 and Landsat 8 in the estimation of boreal forest canopy cover and leaf area index. *Remote Sensing of Environment*, *195*, 259-274. https://doi.org/10.1016/J.RSE.2017.03.021

Landis, J.R., Koch, G.G., 1977. The Measurement of Observer Agreement for Categorical Data. *Biometrics, 33*(1), 159-174. https://doi.org/10.2307/2529310

Lecina-Diaz, J., Martínez-Vilalta, J., Alvarez, A., Vayreda, J., Retana, J., 2021. Assessing the Risk of Losing Forest Ecosystem Services Due to Wildfires. *Ecosystems*, *24*(7), 1687-1701. https://doi.org/10.1007/s10021-021-00611-1

Li, S., Fang, H., Zhang, Y., Wang, Y., 2022. Comprehensive evaluation of global CI, FVC, and LAI products and their relationships using high-resolution reference data. *Science of Remote Sensing*, *6*, 100066. https://doi.org/10.1016/J.SRS.2022.100066

Lloret, F., Pausas, J.G., Vilá, J., 2003. Responses of Mediterranean plant species to different fire frequencies in Garraf Natural Park (Catalonia, Spain): field observations and modelling predictions. *Plant Ecology, 167,* 223-235. https://doi.org/10.1023/A:1023911031155

Maren, E., Gesa, C., Schwanitz, C., Heinken, T., 2023. Early natural regeneration of trees after a forest fire in a Central European Scots pine forest: Forest management, fire severity, and distance are important. *Ecology and Forest Management, 539*, 120999. https://doi.org/10.1016/j.foreco.2023.120999

Martín-Alcón, S., Coll, L., 2016. Unraveling the relative importance of factors driving post-fire regeneration trajectories in non-serotinous Pinus nigra forests. *Forest Ecology and Management, 361*, 13-22. https://doi.org/10.1016/j.foreco.2015.11.006

Martínez, S., Chuvieco, E., Aguado, I., Salas, J., 2017. Severidad y regeneración en grandes incendios forestales: análisis a partir de series temporales de imágenes Landsat. *Revista de Teledetección*, *49*, 17-32. https://doi.org/10.4995/raet.2017.7182

Miller, J.D., Thode, A.E., 2007. Quantifying burn severity in a heterogeneous landscape with a relative version of the delta Normalized Burn Ratio (dNBR). *Remote Sensing of Environment*, 109, 66- 80. https://doi.org/10.1016/j.rse.2006.12.006

Montorio, R., Pérez-Cabello, F, Hoffrén, R., Iranzo, C., 2024. Trends in Wildfire Burn Severity in Aragon, Spain. 13th EARSeL Workshop on Forest Fires 2024. Remote Sensing of Forest Fires: Lessons Learned and Future Challenges Under a Changing Climate. Milan, 19th-20th September 2024. www.edizioni.cnr.it ISBN 978 88 8080 643 1. 1985-2020

Moreno, M., Bertolín, C., Arlanzón, D., Ortiz, P., Ortiz, R., 2023. Climate change, large fires, and cultural landscapes in the mediterranean basin: An analysis in southern Spain. *Heliyon*, *9*(6), 1-19. https://doi.org/10.1016/j.heliyon.2023.e16941

Moya, D., González-De Vega, S., Lozano, E., García-Orenes, F., Mataix-Solera, J., Lucas-Borja, M.E., de las Heras, J., 2019. The burn severity and plant recovery relationship affect the biological and chemical soil properties of Pinus halepensis Mill. stands in the short and mid-terms after wildfire. J. Environ. Manage. 235, 250-256. https://doi.org/10.1016/j.jenvman.2019.01.029

Muñoz-Rojas, M., Pereira, P., 2020. Editorial: Fire in the environment. *Journal of Environmental Management, 253*, 109703. https://doi.org/10.1016/J.JENVMAN.2019.109703

Ne'eman, G., Goubitz, S., Nathan, R., 2004. Reproductive traits of Pinus halepensis in the light of fire - A critical review. *Plant Ecology*, *171*(1-2), 69-79. https://doi.org/10.1023/B:VEGE.0000029380.04821.99

Parra, A., Moreno, J.M., 2018. Drought differentially affects the post-fire dynamics of seeders and resprouters in a Mediterranean shrubland. *Science of the Total Environment*, *626*, 1219-1229. https://doi.org/10.1016/J.SCITOTENV.2018.01.174

Pausas, J.G., 2012. Incendios Forestales. Una visión desde la Ecología. Madrid: CSIC. *Catarata*. https://doi.org/10.1016/j.rse.2013

Pausas, J.G., Bradstock, R.A., Keith, D.A., Keeley, J.E., Hoffman, W., Kenny, B., Lloret, F., Trabaud, L., 2004. Plant functional traits in relation to fire in crown-fire ecosystems. *Ecology*, *85*(4), 1085-1100. https://doi.org/10.1890/02-4094

Pausas, J.G., Keeley, J.E., Schwilk, D.W., 2017. Flammability as an ecological and evolutionary driver. *Journal of Ecology*, *105*(2), 289-297. https://doi.org/10.1111/1365-2745.12691

Pérez-Cabello, F., 2002. Paisajes forestales y fuego en el prepirineo occidental oscense. Un modelo regional de reconstrucción ambiental, Serie Investigación. ed. Publicaciones del Consejo de Protección de la naturaleza de Aragón.

Pettorelli, N., Vik, J.O., Mysterud, A., Gaillard, J.M., Tucker, C.J., Stenseth, N.C., 2005. Using the satellite-derived NDVI to assess ecological responses to environmental change. *Trends in Ecology and Evolution*, *20*(9), 503-510. https://doi.org/10.1016/j.tree.2005.05.011

Pu, J., Yan, K., Roy, S., Zhu, Z., Rautiainen, M., Knyazikhin, Y., Myneni, R.B., 2024. Sensor-independent LAI/FPAR CDR: Reconstructing a global sensor-independent climate data record of MODIS and VIIRS LAI/FPAR from 2000 to 2022. *Earth System Science Data*, *16*(1), 15-34. https://doi.org/10.5194/ESSD-16-15-2024

Ramos, M., Soares, R., 2004. Análisis comparativo entre los incendios forestales en Monte Alegre, Brasil y Pinar del Río, Cuba. *Floresta*, *34*(2), 101-110.

Retana, J., Arnan, X., Arianoutsou, M., Barbati, A., Kazanis, D., Rodrigo, A., 2012. Post-Fire Management of Non-Serotinous Pine Forests. In: F. Moreira, M. Arianoutsou, P. Corona, J. De las Heras (eds.), *Post-Fire Management and Restoration of Southern European Forests*. Managing Forest Ecosystems, vol 24. Springer, Dordrecht. https://doi.org/10.1007/978-94-007-2208-8_7

Richards, J.A., 1999. Remote Sensing Digital Image Analysis: An Introduction. Springer-Verlag, Berlin, Germany, 240. https://doi.org/10.1007/978-3-662-03978-6

Rivas-Martínez, S., 1987. Memoria del mapa de series de vegetación de España. ICONA. Madrid.

Rogan, J., Chen, D.M., 2004. Remote sensing technology for mapping and monitoring land-cover and land-use change. *Progress in Planning*, *61*(4), 301-325. https://doi.org/10.1016/S0305-9006(03)00066-7

Ruffault, J., Curt, T., Moron, V., Trigo, R. M., Mouillot, F., Koutsias, N., Pimont, F., Martin-StPaul, N., Barbero, R., Dupuy, J.L., Russo, A., Belhadj-Khedher, C., 2020. Increased likelihood of heat-induced large wildfires in the Mediterranean Basin. *Scientific Reports*, *10*(1), 1-9. https://doi.org/10.1038/s41598-020-70069-z

Santana, V.M., Baeza, M.J., Maestre, F.T., 2012. Seedling establishment along post-fire succession in Mediterranean shrublands dominated by obligate seeders. *Acta Oecologica*, *39*, 51-60. https://doi.org/10.1016/j.actao.2011.12.001

Shanmuga, R., Vani, K., 2024. Vegetation change detection and recovery assessment based on post-fire satellite imagery using deep learning. *Scientific Reports*, *14*(1), 1-23. https://doi.org/10.1038/s41598-024-63047-2

Shvetsov, E.G., Kukavskaya, E.A., Buryak, L.V., Barrett, K., 2019. Assessment of post-fire vegetation recovery in Southern Siberia using remote sensing observations. *Environmental Research Letters*, *14*(5), 055001. https://doi.org/10.1088/1748-9326/AB083D

Simonetti, D., Simonetti, E., Szantoi, Z., Lupi, A., Eva, H.D., 2015. First Results from the Phenology-Based Synthesis Classifier Using Landsat 8 Imagery. *IEEE Geoscience and Remote Sensing Letters*, *12*(7), 1496-1500. https://doi.org/10.1109/LGRS.2015.2409982

Vallejo R., Serrasolses, I., Alloza, J.A, Baeza, M., 2009. Long-term restoration strategies and techniques". In: A. Cerdá y P. Robichaud (eds.), *Fire Effects on Soils and Restoration Strategies*. Enfield, Science Publishers, pp. 373-398.

Vayreda, J., Martinez-Vilalta, J., Gracia, M., Canadell, J.G., Retana, J., 2016. Anthropogenic-driven rapid shifts in tree distribution lead to increased dominance of broadleaf species. *Global Change Biology*, *22*(12), 3984-3995. https://doi.org/10.1111/gcb.13394

Vermote, E.F., Tanré, D., Deuzé, J.L., Herman, M., Morcrette, J.J., 1997. Second simulation of the satellite signal in the solar spectrum, 6s: an overview. *IEEE Transactions on Geoscience and Remote Sensing*, *35*(3), 675-686. https://doi.org/10.1109/36.581987

Viana-Soto, A., Aguado, I., Salas, J., García, M., 2020. Identifying Post-Fire Recovery Trajectories and Driving Factors Using Landsat Time Series in Fire-Prone Mediterranean Pine Forests. *Remote Sens., 12*, 1499. https://doi.org/10.3390/rs12091499

Vogelmann, J.E., Xian, G., Homer, C., Tolk, B., 2012. Monitoring gradual ecosystem change using Landsat time series analyses: Case studies in selected forest and rangeland ecosystems. *Remote Sensing of Environment*, *122*, 92-105. https://doi.org/10.1016/J.RSE.2011.06.027

Wagtendonk, J.W., Root, R.R., Key, C.H., 2004. Comparison of AVIRIS and Landsat ETM+ detection capabilities for burn severity. *Remote Sensing of Environment, 92*, 397-408. https://doi.org/10.1016/j.rse.2003.12.015

Wilson, R.T., 2013. Py6S: A Python interface to the 6S radiative transfer model. *Computers & Geosciences*, *51,* 166-171. https://doi.org/10.1016/j.cageo.2012.08.002

Woodgate, W., Phinn, S., Devereux, T., Aryal, R.R., 2024. Bushfire recovery at a long-term tall eucalypt flux site through the lens of a satellite: Combining multi-scale data for structural-functional insight. *Remote Sensing of Environment*, *317*, 114530. https://doi.org/10.1016/J.RSE.2024.114530

Wulder, A.M., Roy, D.P., Radeloff, V.C., Loveland, T.R, Anderson, M.C., Johnson, D., Healey, S.; Zhu, Z., Scambos, T.A., Pahlevan, N., Hansen, M., Gorelick, N, Crawford, C.J., Masek, J., Hermosilla, T, White, J.C., Belward, A.S., Schaaf, C., Woodcock, C.E., Huntington, J.L., Lymburner, L., Hostert, P., Gao, F., Lyapustin, A., Pekel, J., Strobl, P., Cook, B.D. 2022. Fifty years of Landsat science and impacts. *Remote Sensing of Environment*, *280*, 2-20. https://doi.org/10.1016/j.rse.2022.113195

Xuan, G., Zhang, W., Chai, P., 2001. EM algorithms of Gaussian mixture model and hidden Markov model. *Proceedings 2001 International Conference on Image Processing*. Thessaloniki, Greece, vol.1, 145-148. https://doi.org/10.1109/ICIP.2001.958974